



Cite this: *Dalton Trans.*, 2017, **46**, 16004

Received 1st September 2017,  
Accepted 4th October 2017

DOI: 10.1039/c7dt03243a

rsc.li/dalton

The condensation reaction of 2-aminobenzenethiols and 3-amino-pyrazinethiols with 2-amino-6-fluoro-*N*-methylpyridinium triflate afforded thioether derivatives that were found to undergo Smiles rearrangement and cyclocondensation with sulphur monochloride to yield new hybrid 1,4-thiazine-1,2,3-dithiazolyl cations. The synthesized cations were readily reduced to the corresponding stable neutral radicals with spin densities delocalized over both 1,4-thiazinyl and 1,2,3-dithiazolyl moieties.

The heterocyclic benzo-1,4-thiazine, or simply phenothiazine, was first synthesized more than a century ago.<sup>1</sup> Over the years, phenothiazine and its numerous derivatives have been broadly examined, largely due to their biological activity and use as antipsychotic drugs.<sup>2</sup> The widespread interest in the medicinal chemistry of phenothiazine has also spurred the development of a variety of synthetic protocols for the preparation of new compounds. Of topical interest is the Smiles rearrangement,<sup>3</sup> an intramolecular nucleophilic *ipso*-substitution reaction, which has found extensive use in the preparation of a number of phenothiazine-based heterocycles.<sup>4</sup>

The application potential of phenothiazines extends beyond pharmaceuticals and they can also be used as building blocks for functional materials. This stems from the ability of phenothiazine and its derivatives to undergo facile one-electron oxidation to persistent radical cations,<sup>5</sup> which have been characterized by both EPR spectroscopy and X-ray crystallography.<sup>6,7</sup> In recent years, the materials-oriented research has shifted the synthetic focus towards linked and fused oligomers of phenothiazine as well as phenothiazine-based polymers because of their applicability as switchable molecules, photosensitizers, cathode-active materials, and organic open-shell polymers to name a few.<sup>8</sup>

Department of Chemistry, NanoScience Centre, P.O. Box 35, FI-40014 University of Jyväskylä, Finland. E-mail: aaron.m.mailman@jyu.fi, heikki.m.tuononen@jyu.fi

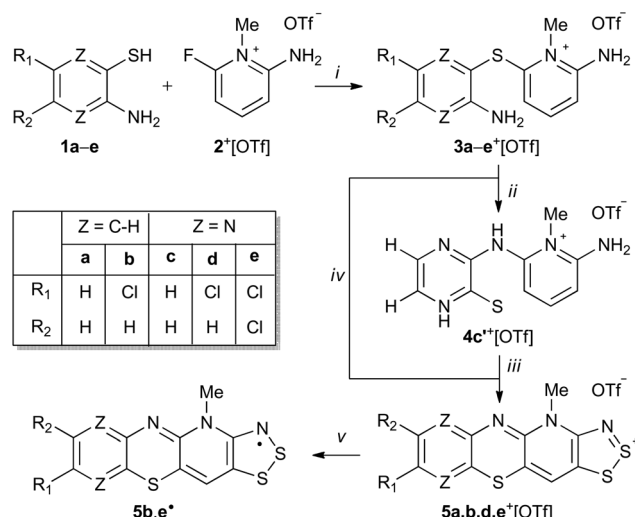
† Electronic supplementary information (ESI) available: Full details of synthetic, spectroscopic, computational, and crystallographic work. CCDC 1519804–1519808, 1536800 and 1536801. For ESI and crystallographic data in CIF or other electronic format see DOI: 10.1039/c7dt03243a

## Synthesis of new hybrid 1,4-thiazinyl-1,2,3-dithiazolyl radicals via Smiles rearrangement†

Petra Vasko, Juha Hurmalainen, Akseli Mansikkamäki, Anssi Peuronen, Aaron Mailman\* and Heikki M. Tuononen \*

Regardless of the wealth of data on cation radicals of phenothiazine, little is known about neutral phenothiazinyls even though these radicals were reported in the early 1960s.<sup>9</sup> The majority of data on phenothiazinyl radicals are limited to spectroscopic studies and, to the best of our knowledge, there are no reports of X-ray crystallographic investigations. This is surprising considering that the related heterocyclic 1,2-thiazinyl radicals have been thoroughly characterized despite their persistent nature.<sup>10</sup> Consequently, in an effort to extend the chemistry of neutral phenothiazinyl derivatives, we report the use of the Smiles rearrangement reaction to prepare new stable radicals  $5^{\bullet}$  that fuse the 1,4-thiazinyl and 1,2,3-dithiazolyl moieties into a single framework (Scheme 1).

The molecular scaffold in radicals  $5^{\bullet}$  was chosen because of the wide range of physical and chemical properties of thiazyl-based radicals that make them useful building blocks for



**Scheme 1** Synthesis of neutral radicals  $5^{\bullet}$ . Reagents and general conditions: (i)  $\text{Na}_2\text{CO}_3$ , MeCN, 5 h; (ii) MeCN, sealed vessel, 110 °C; (iii) excess  $\text{S}_2\text{Cl}_2$ , MeCN, reflux, 16 h; (iv) excess  $\text{S}_2\text{Cl}_2$ , MeCN, reflux, 16 h; (v) excess  $\text{Me}_8\text{Fc}$ , MeCN. Highest yields obtained:  $4\text{c}^{\bullet}[\text{OTf}]$  79%,  $5\text{a}^{\bullet}[\text{OTf}]$  2%,  $5\text{b}^{\bullet}[\text{OTf}]$  43%,  $5\text{d}^{\bullet}[\text{OTf}]$  48%,  $5\text{e}^{\bullet}[\text{OTf}]$ , 78%,  $5\text{b}^{\bullet}$  81%, and  $5\text{e}^{\bullet}$  70%.



molecular materials, both as free species and as coordinating ligands.<sup>11</sup> While the first examples of closely related hybrid 1,2,3-dithiazolo-1,2,4-thiadiazinyl radicals have only been reported in the last few years,<sup>12</sup> *N*-alkylpyridinium bridged bis-1,2,3-dithiazolyls and their selenium variants, with mirror plane symmetry, have been extensively explored.<sup>11b,13</sup> Many of these radicals were initially pursued as possible single component molecular conductors. However, their diverse magnetic properties, including ferromagnetic ordering, are notable compared to related classes of light atom molecular radicals such as nitroxides, triazinyls, and verdazyls.<sup>11b</sup> Thus, the pursuit of new molecular thiazyl radicals continues to attract considerable attention, which has now lead us to explore new extended aromatic systems based on the synthetically useful *N*-alkylpyridinium template.

The condensation reaction of 2-aminobenzenethiols (**1a,b**) and 3-aminopyrazinethiols (**1c,d,e**) with 2-amino-6-fluoro-*N*-methylpyridinium triflate (**2<sup>+</sup>[OTf]**)<sup>12</sup> in the presence of excess anhydrous  $\text{Na}_2\text{CO}_3$  in acetonitrile (MeCN) afforded *N*-methylpyridinium thioether salts **3a–e<sup>+</sup>[OTf]** (Scheme 1, step i).

Recrystallization of **3<sup>+</sup>[OTf]** from appropriate solvents gave analytically pure crystalline solids, which were characterized by IR and NMR ( $^1\text{H}$ ,  $^{13}\text{C}\{^1\text{H}\}$ ) spectroscopy as well as by single crystal X-ray diffraction analysis (for **3c<sup>+</sup>[OTf]**, Fig. 1a).

It was anticipated that the salts **3<sup>+</sup>[OTf]** would undergo S  $\rightarrow$  N Smiles rearrangement (SR) reaction by intramolecular nucleophilic *ipso*-substitution at the thioether bond of the *N*-methylpyridinium, affording *N*-substituted derivatives **4<sup>+</sup>[OTf]** (Scheme 1, step ii). After screening different reaction conditions on NMR scale, an essentially quantitative reaction was realised for **3c<sup>+</sup>[OTf]** but only after heating for 8 days at 80 °C. The purported SR reaction was performed on preparative scale in a sealed pressure vessel at 110 °C in MeCN, which gave an isolated product in high yield (80%) only after 40 h.

Single crystal X-ray diffraction analysis confirmed the heavy atom (non-hydrogen) connectivity of **4c<sup>+</sup>[OTf]**, but instead of the expected thiol, the product was found to be the tautomeric pyrazinethione derivative **4c'<sup>+</sup>[OTf]** (Fig. 1b). The  $^1\text{H}$ -NMR

spectrum of the product (in anhydrous  $\text{CD}_3\text{CN}$ ) revealed that the signals for the pyridinium  $-\text{NH}_2$  and pyrazine C–H protons are distinctively downfield shifted compared to **3c<sup>+</sup>[OTf]** and the appearance of a broad singlet at  $\delta$  9.60 ppm is tentatively assigned to the pyrazine  $-\text{NH}$  proton (N3 in Fig. 1b). It is notable that the  $^1\text{H}$ -NMR spectrum of **4c'<sup>+</sup>[OTf]** does not show an observable signal for the bridging  $-\text{NH}$  group (N5 in Fig. 1b).

The lack of similar reactivity for the other thioether salts **3<sup>+</sup>[OTf]** even under more forceful conditions led us to perform a density functional study of the reaction mechanism at the PBE1PBE-IEFPCM/def2-TZVP level of theory. The results of computational investigations are summarized in Fig. 2 for two representative systems, **3a<sup>+</sup>** and **3c<sup>+</sup>**.

It is evident from the computed data (Fig. 2) that the initial reaction pathway is similar for both **3a<sup>+</sup>** and **3c<sup>+</sup>**. It was assumed that the SR reaction begins with an intramolecular nucleophilic attack of the benzo/pyrazine  $-\text{NH}_2$  group to form a cationic Meisenheimer complex **Int1**.<sup>3</sup> This step has a very high activation barrier, **TS1**, in agreement with experimental observations. Furthermore, the formation of **4a<sup>+</sup>** and **4c<sup>+</sup>** is in both cases an essentially energy neutral process. However, what drives the SR reaction forward in the case of **3c<sup>+</sup>** is the possibility for **4c<sup>+</sup>** to tautomerize to the experimentally characterized form **4c'<sup>+</sup>**, which renders the overall reaction exergonic by 43 kJ mol<sup>-1</sup>. In this respect, it is surprising that no SR reaction was realized for **3d<sup>+</sup>** and **3e<sup>+</sup>** even though these derivatives are also able to tautomerize to the corresponding pyrazinethiones. A computational analysis of their reaction pathways showed that the formation of both **4d<sup>+</sup>** and **4e<sup>+</sup>** is exergonic, though only by 20 and 11 kJ mol<sup>-1</sup>, respectively. Hence, the SR

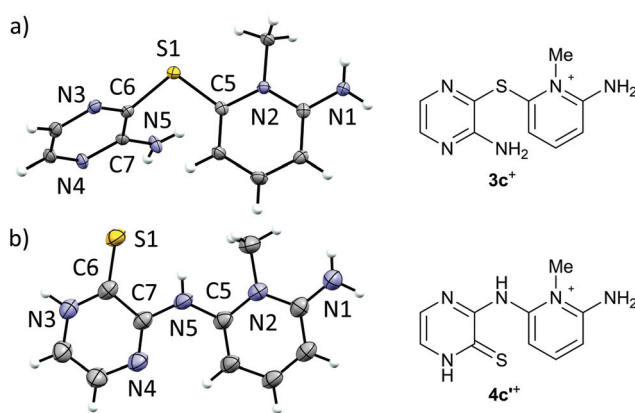


Fig. 1 ORTEP plots (left, thermal ellipsoids at 50% probability) and line drawings (right) of the cations in (a) **3c<sup>+</sup>[OTf]** and (b) **4c<sup>+</sup>[OTf]**.

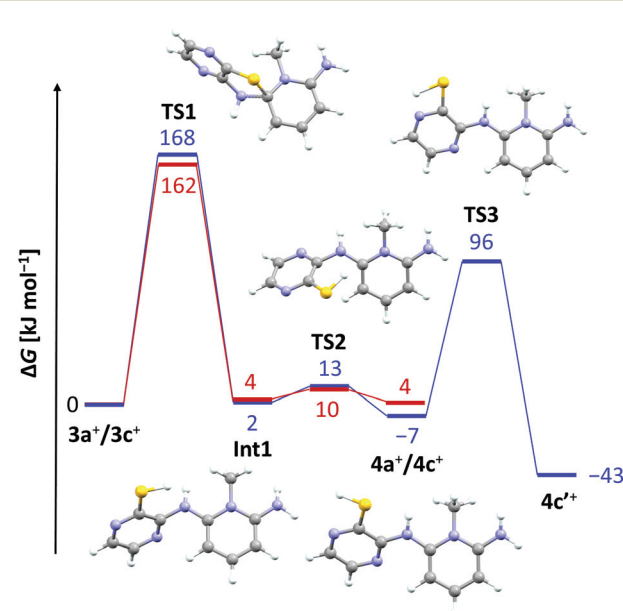


Fig. 2 Reaction coordinate diagram (PBE1PBE-IEFPCM/def2-TZVP) for the Smiles rearrangement reaction of **3a<sup>+</sup>** (red) and **3c<sup>+</sup>** (blue). For clarity, the structures of intermediates and transition states are only shown for the pathway from **3c<sup>+</sup>** to **4c'<sup>+</sup>**.



reaction becomes less-favoured for each chlorine substituent added, making **4c**<sup>+</sup> the most favourable product of the different derivatives **a–e** considered. Consequently, **4c**<sup>+</sup> is the only species generated under the experimental reaction conditions.

Having confirmed the identity of **4c**<sup>+</sup>[OTf], its cyclocondensation with excess S<sub>2</sub>Cl<sub>2</sub> was performed by refluxing the reactants in MeCN for 16 h (Scheme 1, step iii). Low-resolution positive ion electrospray ionization mass spectrometry (+ESI-MS) showed that the main products from the reaction were the salt **5c**<sup>+</sup>[OTf] and the doubly chlorinated analogue **5e**<sup>+</sup>[OTf]. Repeated syntheses confirmed that the **5c**<sup>+</sup>[OTf] : **5e**<sup>+</sup>[OTf] ratio is variable and does not depend on the reaction conditions in any obvious manner. However, the chlorinated product **5e**<sup>+</sup>[OTf] could be crystallised from the reaction mixture using MeCN, affording a small amount of purple blocks. Unsatisfied with the low yield of **5e**<sup>+</sup>[OTf], we attempted the direct reaction of S<sub>2</sub>Cl<sub>2</sub> with thioether **3e**<sup>+</sup>[OTf] that already contains an appropriate substitution of chlorine on the pyrazine ring to potentially afford another route to **5e**<sup>+</sup>[OTf] (Scheme 1, step iv). To our delight, **5e**<sup>+</sup>[OTf] was obtained in good isolated yield (78%) as confirmed by IR spectroscopy and +ESI-MS.

To explore the scope of this alternative pathway to **5**<sup>+</sup>[OTf], the reactivity of **3a**<sup>+</sup>[OTf], **3b**<sup>+</sup>[OTf], and **3d**<sup>+</sup>[OTf] with S<sub>2</sub>Cl<sub>2</sub> was also investigated. In the case of **3a**<sup>+</sup>[OTf], +ESI-MS suggested that the product is a mixture of the non-chlorinated salt **5a**<sup>+</sup>[OTf] with its chlorinated analogues containing one or more chlorine atoms. Hence, **5a**<sup>+</sup>[OTf] was obtained in very low isolated yield (2%). Condensation reactions of S<sub>2</sub>Cl<sub>2</sub> with aromatic amines containing an unsubstituted *para*-position (or those containing a good leaving group) are well-known to undergo simultaneous chlorination. Consequently, the reaction of S<sub>2</sub>Cl<sub>2</sub> with the chlorinated species **3b**<sup>+</sup>[OTf] and **3d**<sup>+</sup>[OTf] was found to offer a practical route to derivatives **5b**<sup>+</sup>[OTf] and **5d**<sup>+</sup>[OTf] without further chlorination, albeit in moderate yield (43 and 48%, respectively). This further demonstrates that SR and cyclocondensation can take place concomitantly rather than sequentially, providing another route to different derivatives of **5**<sup>+</sup>[OTf].

Cyclic voltammetry performed on solutions of **5**<sup>+</sup>[OTf] in MeCN (with 0.1 M *n*-Bu<sub>4</sub>NPF<sub>6</sub> as the supporting electrolyte) displayed a reversible +1/0 redox couple with  $E_{1/2} = 0.031$  V and 0.220 V (vs. SCE) for **5b**<sup>+</sup>[OTf] and **5e**<sup>+</sup>[OTf], respectively. The cathodic shift in  $E_{1/2}$  indicates that the heterocyclic aromatic substituent affects the electrochemical behaviour of the cations by altering the energy of their lowest unoccupied molecular orbital. This provides opportunities to fine-tune the electronic properties of the cations **5**<sup>+</sup> through careful choice of substituents. Furthermore, the  $E_{1/2}$  values for **5b**<sup>+</sup>[OTf] and **5d**<sup>+</sup>[OTf] clearly demonstrate that octamethylferrocene (Me<sub>8</sub>Fc) is a suitable reducing agent for both cations. The cyclic voltammetry measurements also revealed that the 0/–1 redox couple is irreversible for **5e**<sup>+</sup>[OTf], while **5b**<sup>+</sup>[OTf] appears to undergo significant decomposition under the same conditions. The estimated  $E_{cell}$  of **5e**<sup>+</sup>[OTf] is 0.720 V, which is smaller than those of related bisdithiazolyl radicals

( $E_{cell} = 0.851$  V) but comparable to analogous bisthiaselenazolyls ( $E_{cell} = 0.745$  V).<sup>14</sup> Reduction of **5b**<sup>+</sup>[OTf] and **5e**<sup>+</sup>[OTf] was performed by slow diffusion of a degassed MeCN solution of the salt through a medium porosity sintered glass frit into a similar degassed MeCN solution of excess of Me<sub>8</sub>Fc. This afforded the radicals **5b**<sup>·</sup> and **5e**<sup>·</sup> as analytically pure crystalline solids (Scheme 1, step v). In the case of **5b**<sup>·</sup>, crystals suitable for single crystal X-ray diffraction were obtained as small lustrous bronze blocks. The crystal structure of **5b**<sup>·</sup> belongs to the centrosymmetric monoclinic space group *P2<sub>1</sub>/c*. The asymmetric unit consists of two essentially coplanar radicals in *trans*-cofacial arrangement (Fig. 3) with the shortest intermolecular C···C interactions very close to the sum of van der Waals radii.<sup>15</sup> This suggests that the radicals are not strongly interacting in the solid state. The radicals in the asymmetric unit of **5b**<sup>·</sup> and those related to them by an inversion centre form  $\pi$ -stacked motifs that are arranged in a herringbone pattern similar to those typically observed for related bisdithiazolyl radicals.<sup>14,16</sup>

The electronic structures of **5b**<sup>·</sup> and **5e**<sup>·</sup> were investigated by a combination of computational (PBE1PBE/def2-TZVP) methods and EPR spectroscopy. The calculations showed that the singly occupied molecular orbital and the spin density of **5**<sup>·</sup> are delocalized over the molecular backbone (Fig. 4). Specifically, natural population analysis assigned 40 and 55% of the  $\alpha$ -spin density of **5b**<sup>·</sup> on the 1,4-thiazinyl and 1,2,3-dithiazolyl moieties, respectively; the spin distribution of **5e**<sup>·</sup> is slightly more localised on the 1,2,3-dithiazolyl moiety. Consequently, the radicals **5** can be considered hybrids of 1,4-thiazinyls and 1,2,3-dithiazolyls, which underlines the fact that the line drawing in Scheme 1 is an oversimplified picture of their electronic structure. In this respect, population analyses of **5b**<sup>+</sup> and **5d**<sup>+</sup> showed that the sulphur atom on the 1,4-thiazine ring is the single most positively charged nucleus in the structures. However, the shortest anion···cation contacts in crystal structures of **5b**<sup>+</sup>[OTf] and **5d**<sup>+</sup>[OTf] involve the two sulphur atoms on the 1,2,3-dithiazolyl moiety.

The room-temperature EPR spectrum of **5b**<sup>·</sup> in CH<sub>2</sub>Cl<sub>2</sub> (Fig. 5a) consists of an eight line pattern with  $g = 2.0071$  and no fine-structure. A good simulation of the spectrum was obtained by using hyperfine couplings (hfcs) to the nitrogen nuclei in the dithiazolyl ( $a_{N1} = 0.383$  mT) and thiazyl

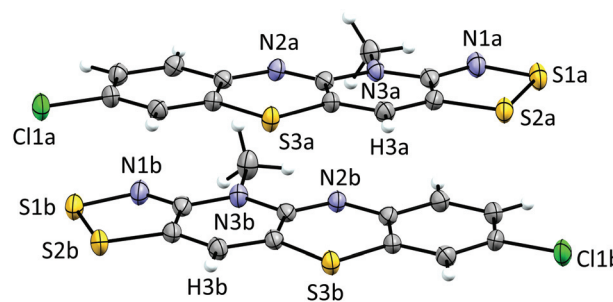
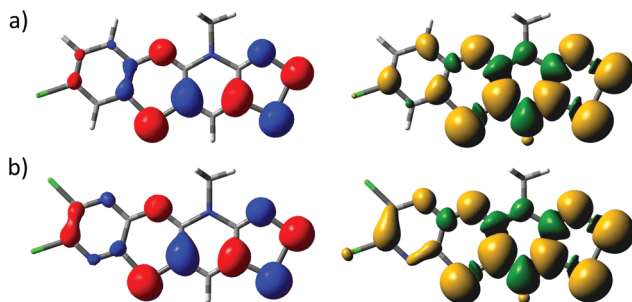
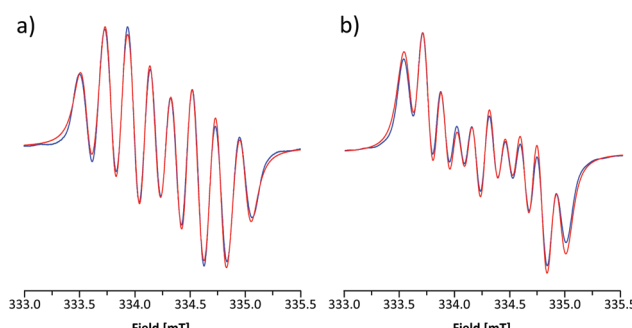


Fig. 3 ORTEP plot of the asymmetric unit of **5b**<sup>·</sup> (thermal ellipsoids at 50% probability).





**Fig. 4** Isosurface plots of the SOMOs ( $\pm 0.04$ , left) and spin densities ( $\pm 0.001$ , right) of (a) **5b\*** and (b) **5e\***.



**Fig. 5** Experimental (blue) and simulated (red) X-band EPR spectra of  $\text{CH}_2\text{Cl}_2$  solutions of (a) **5b\*** and (b) **5e\*** at room temperature. The simulations used Voigtian functions with Gaussian/Lorenzian peak-to-peak line widths (mT) of 0.067/0.092 and 0.090/0.087 for **5b\*** and **5d\***, respectively.

( $a_{N2} = 0.224$  mT) rings as well as to one hydrogen atom at the basal position ( $a_{H3} = 0.213$  mT). The assignment of hfcs was based on a computational analysis of **5b\*** ( $a_{N1} = 0.304$ ,  $a_{N2} = 0.206$ , and  $a_{H3} = 0.375$  mT), which also suggested the presence of smaller couplings to hydrogen nuclei ( $a_H \approx -0.070$  mT) and the nitrogen atom on the *N*-methylpyridinium ring ( $a_{N3} = -0.052$  mT). However, the broad spectral line width did not allow the explicit consideration of these hfcs in simulations for which reason they were treated indirectly by adjusting the line shape. The EPR spectrum of **5e\*** is similar to that of **5b\*** with  $g = 2.0059$ . The spectrum consists of ten broad lines and a good simulation of it was obtained by using hfcs to the nitrogen nuclei in the dithiazolyl ( $a_{N1} = 0.484$  mT) and thiazyl ( $a_{N2} = 0.169$  mT) rings as well as to the hydrogen atom at the basal position ( $a_{H3} = 0.197$  mT). This view is well supported by calculations ( $a_{N1} = 0.356$ ,  $a_{N2} = 0.153$ , and  $a_{H3} = 0.332$  mT), which also revealed minute coupling of the unpaired electron to the pyrazine nitrogen atoms.

Having shown that the SR reaction offers a viable route to **5\***, the scope of the two established pathways was examined further. Considering the utilization of **5\*** in practical applications, the stability of the radicals is of particular importance. In this context, delocalization of the spin density on the 1,4-thiazinyl moiety is desired. Thus, we chose the quinoxaline

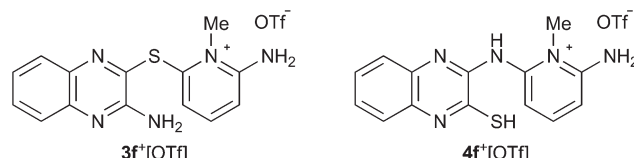


Chart 1

derivative **4f<sup>+</sup>[OTf]** as our primary target (Chart 1). The synthesis of **3f<sup>+</sup>[OTf]** from 3-aminoquinoxalinethiol and 2-amino-6-fluoro-N-methylpyridinium trifluoromethanesulfonate was performed as described in Scheme 1 (step i). To our delight, **3f<sup>+</sup>[OTf]** undergoes the SR reaction (step ii) extremely easily as some **4f<sup>+</sup>[OTf]** was formed even during recrystallization of **3f<sup>+</sup>[OTf]**. Complete conversion required refluxing **3f<sup>+</sup>[OTf]** in MeCN for 6 h, giving **4f<sup>+</sup>[OTf]** in high isolated yield (80%). The identity of **3f<sup>+</sup>[OTf]** and **4f<sup>+</sup>[OTf]** was confirmed by both NMR spectroscopy and single-crystal X-ray crystallography. This demonstrates that, when using appropriate 3-aminoquinoxalinethiols, the SR reaction is an extremely viable pathway for the synthesis of salts **4<sup>+</sup>[OTf]**, which yield the corresponding stable neutral radicals **5<sup>+</sup>** after ring closure and reduction.

## Conclusions

In this communication, we have shown that the Smiles rearrangement reaction, either followed by cyclocondensation or performed concurrently with it, offers a viable and modifiable route to a new class of hybrid 1,4-thiazine-1,2,3-dithiazolylium salts **5<sup>+</sup>[OTf]**, which can be readily reduced to yield the corresponding neutral radicals **5<sup>+</sup>** with spin densities delocalized over both 1,4-thiazinyl and 1,2,3-dithiazolyl moieties. Future work will focus on the characterisation of transport properties of **5<sup>+</sup>** and related radicals, along with the exploration of their coordination chemistry. This will provide opportunities for the design of molecular materials that may exhibit novel physical properties.

## Conflicts of interest

There are no conflicts to declare.

## Acknowledgements

This work was financially supported by the University of Jyväskylä, the Academy of Finland (projects 253907 and 289172) and the European Union's H2020 programme (under the Marie Skłodowska-Curie grant agreement 659123). We thank Laboratory Technicians Johanna Lind and Elina Hautakangas for running the +ESI-MS and EA measurements, respectively.



## Notes and references

1 A. Berthsen, *Ber. Dtsch. Chem. Ges.*, 1883, **16**, 2896.

2 See, for example: (a) A. Jaszczyszyn, K. Gasiorowski, P. Swiatek, W. Malinka, K. Cieslik-Boczula, J. Petrus and B. Czarnik-Matusewicz, *Pharmacol. Rep.*, 2012, **64**, 16; (b) M. J. Ohlow and B. Moosmann, *Drug Discovery Today*, 2011, **16**, 119; (c) G. Sudeshna and K. Parimal, *Eur. J. Pharmacol.*, 2010, **648**, 6; (d) M. Wainwright and L. Amaral, *Trop. Med. Int. Health*, 2007, **10**, 501; (e) *Phenothiazines and 1,4-Benzothiazines. Chemical and Biomedical Aspects (Bioactive Molecules, Vol. 4)*, ed. R. R. Gupta, Elsevier, Amsterdam, 1988.

3 W. E. Truce, E. M. Kreider and W. W. Brand, *Org. React.*, 1970, **18**, 99.

4 See, for example: (a) B. Morak-Młodawska, K. Pluta, M. Latocha and M. Jeleń, *Med. Chem. Res.*, 2016, **25**, 2425; (b) M. Jeleń, K. Pluta, K. Suwińska, B. Morak-Młodawska, M. Latocha and A. Shkurenko, *J. Mol. Struct.*, 2015, **1099**, 10; (c) N. Gautam, A. Guleria, M. K. Sharma, S. K. Gupta, A. Goyal and D. C. Gautam, *Curr. Bioact. Compd.*, 2014, **10**, 189; (d) Y. Zhao, Y. Bai, Q. Zhang, Z. Chen, Q. Dai and C. Ma, *Tetrahedron Lett.*, 2013, **54**, 3253; (e) M. Jeleń, K. Suwińska, C. Besnard, K. Pluta and B. Morak-Młodawska, *Heterocycles*, 2012, **85**, 2281; (f) B. Morak-Młodawska, K. Suwińska, K. Pluta and M. Jeleń, *J. Mol. Struct.*, 2012, **1015**, 94; (g) N. Gautam, K. Goyal, O. Saini, A. Kumar and D. C. Gautam, *J. Fluorine Chem.*, 2011, **132**, 420.

5 (a) F. Kehrmann and L. Diserens, *Ber.*, 1915, **48**, 318; (b) R. Pummerer and S. Gassner, *Ber.*, 1913, **46**, 2310.

6 (a) S. C. Blackstock and T. D. Selby, in *Magnetic Properties of Organic Materials*, ed. P. M. Lahti, Marcel Dekker Inc., New York, 1999, p. 165.

7 (a) K. Kozawa and T. Uchida, *Acta Crystallogr., Sect. C: Cryst. Struct. Commun.*, 1993, **49**, 267; (b) K. Kozawa, T. Hoshizaki and T. Uchida, *Bull. Chem. Soc. Jpn.*, 1991, **64**, 2039; (c) K. Kozawa and T. Uchida, *Acta Crystallogr., Sect. C: Cryst. Struct. Commun.*, 1990, **46**, 1006; (d) A. Singhabhandhu, P. D. Robinson, J. H. Fang and W. E. Geiger Jr., *Inorg. Chem.*, 1975, **14**, 318.

8 For recent examples, see: (a) Z.-S. Huang, H. Meier and D. Cao, *J. Mater. Chem. C*, 2016, **4**, 2404; (b) X. Wang, Z. Zhang, Y. Song, Y. Su and X. Wang, *Chem. Commun.*, 2015, **51**, 11822; (c) H. Oka, *Org. Lett.*, 2010, **12**, 448; (d) A. W. Franz, L. N. Popa, F. Rominger and T. J. J. Müller, *Org. Biomol. Chem.*, 2009, **7**, 469; (e) H. Oka, *J. Mater. Chem.*, 2008, **18**, 1927; (f) A. A. Golriz, T. Suga, H. Nishide, R. Berger and J. S. Gutmann, *RSC Adv.*, 2005, **5**, 22947; (g) T. Okamoto, M. Kuratsu, M. Kozaki, K. Hirotsu, A. Ichimura, T. Matsushita and K. Okada, *Org. Lett.*, 2004, **6**, 3493; (h) Z. Gomurashvili and J. V. Crivello, *Macromolecules*, 2002, **35**, 2962.

9 (a) Y. Tsujino, *Tetrahedron Lett.*, 1968, **9**, 4111; (b) C. Jackson and N. K. D. Patel, *Tetrahedron Lett.*, 1967, **8**, 2255; (c) B. C. Gilbert, P. Hanson, R. O. C. Norman and B. T. Sutcliffe, *Chem. Commun.*, 1966, 161; (d) H. J. Shine and E. E. Mach, *J. Org. Chem.*, 1965, **30**, 2130; (e) C. Bodea and I. Silberg, *Nature*, 1963, **198**, 883.

10 (a) M. J. Sienkowska, J. M. Farrar and P. Kaszynski, *Liquid Cryst.*, 2007, **34**, 19; (b) P. Kaszynski, *Molecules*, 2004, **9**, 716; (c) V. Benin and P. Kaszynski, *J. Org. Chem.*, 2000, **65**, 8086.

11 (a) K. E. Preuss, *Coord. Chem. Rev.*, 2015, **289–290**, 49; (b) R. G. Hicks, in *Stable Radicals Fundamentals and Applied Aspects of Odd-Electron Compounds*, ed. R. G. Hicks, John Wiley & Sons Ltd., Wiltshire, 2010, p. 317.

12 S. M. Winter, A. R. Balo, R. J. Roberts, K. Lekin, A. Assoud, P. A. Dube and R. T. Oakley, *Chem. Commun.*, 2013, **49**, 1603.

13 See for example: (a) K. Lekin, K. Ogata, A. Maclean, A. Mailman, S. M. Winter, A. Assoud, M. Mito, J. S. Tse, S. Desgreniers, N. Hirao, P. A. Dube and R. T. Oakley, *Chem. Commun.*, 2016, **52**, 13877; (b) S. M. Winter, S. Hill and R. T. Oakley, *J. Am. Chem. Soc.*, 2015, **137**, 3720; (c) K. Lekin, J. W. L. Wong, S. M. Winter, A. Mailman, P. A. Dube and R. T. Oakley, *Inorg. Chem.*, 2013, **52**, 2188; (d) A. A. Leitch, K. Lekin, S. M. Winter, L. E. Downie, H. Tsuruda, J. S. Tse, M. Mito, S. Desgreniers, P. A. Dube, S. Zhang, Q. Liu, C. Jin, Y. Oshishi and R. T. Oakley, *J. Am. Chem. Soc.*, 2011, **133**, 6051.

14 (a) J. Brusso, S. Derakshan, M. E. Itkis, H. Kleinke, R. C. Haddon, R. T. Oakley, R. W. Reed, J. F. Richardson, C. M. Robertson and L. K. Thompson, *Inorg. Chem.*, 2006, **45**, 10958; (b) L. Beer, J. L. Brusso, R. C. Haddon, M. E. Itkis, R. T. Oakley, R. W. Reed, J. F. Richardson, R. A. Secco and X. Yu, *Chem. Commun.*, 2005, 5745.

15 (a) I. Dance, *New J. Chem.*, 2003, **27**, 22; (b) A. J. Bondi, *J. Phys. Chem.*, 1964, **68**, 441.

16 (a) L. Beer, J. F. Britten, O. P. Clements, R. C. Haddon, M. E. Itkis, K. M. Matkovich, R. T. Oakley and R. W. Reed, *Chem. Mater.*, 2004, **16**, 1564; (b) L. Beer, J. F. Britten, J. L. Brusso, A. W. Cordes, R. C. Haddon, M. E. Itkis, D. S. MacGregor, R. T. Oakley, R. W. Reed and C. M. Robertson, *J. Am. Chem. Soc.*, 2003, **125**, 14394.

